Specific features of the loss of stability during radial displacement of fluid in the Hele–Shaw cell

2008 J. Phys.: Condens. Matter 20 045201

(http://iopscience.iop.org/0953-8984/20/4/045201)

J. Phys.: Condens. Matter **20** (2008) 045201 (8pp) doi:10.1088/0953-8984/20/04/045201

Specific features of the loss of stability during radial displacement of fluid in the Hele–Shaw cell

L M Martyushev and A I Birzina

Institute of Industrial Ecology, Ekaterinburg, Russia

E-mail: mlm@ecko.uran.ru

Received 18 September 2007, in final form 4 December 2007
Published 8 January 2008
Online at stacks.iop.org/JPhysCM/20/045201

Abstract

The study deals with linear analysis of the stability of the interface of a radially displaced fluid (at a constant flow rate or pressure) in the Hele–Shaw cell. As distinct from other studies, the calculations have been performed considering finite size of the system and nonzero viscosity of the displacing fluid. Consequently, earlier results have been considerably refined. An interesting feature—varying sensitivity of the system to perturbations with changing control parameters—has been detected and analyzed. Therefore, this system can be viewed as a specific filter which picks harmonics of certain frequencies out of random mechanical effects and amplifies them.

1. Introduction

The displacement of one fluid by another fluid can be highly unstable. For example, if a less viscous fluid displaces a more viscous one during their horizontal movement between parallel plates spaced a short distance (the Hele–Shaw cell), the interface between the fluids develops a finger-like appearance [1–4]. This phenomenon is extensively studied [2–7] because the regular features observed here are very interesting from the viewpoint of physics of nonequilibrium processes and are sufficiently universal (a similar situation is observed, e.g., during formation of dendrite structures) [4]. An important particular case of the phenomenon in hand is the so-called radial displacement when the displacing fluid flows from the center of the Hele–Shaw cell (figure 1).

This unstable process was described analytically for the first time in [8, 9]. Although the solutions provided the qualitative description of the process, they had some drawbacks. For example, according to the obtained results, the initial circle interface is always stable to small perturbations of the translation type (when interface is displaced from the center as a unit), whereas in experiments, in contrast, this type of instability is very frequent. This contradiction probably is due to the fact that the problem was solved on the assumption of an infinite cell. Furthermore, it was assumed that the pressure p changes abruptly at the interface:

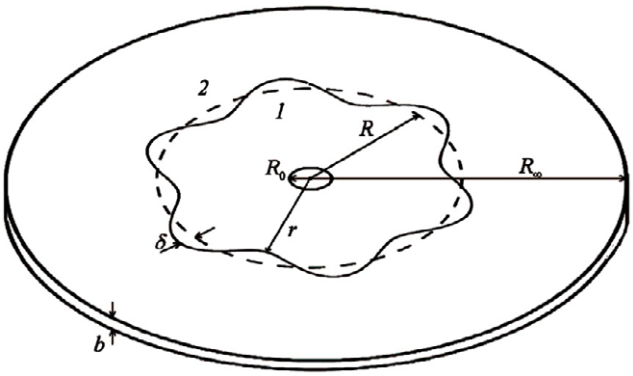

Figure 1. Radial displacement in the Hele–Shaw cell.

$$\Delta p = 2\sigma/b + \sigma K, \tag{1.1}$$

where σ is the surface tension, K is the surface curvature in the motion plane, and b is the cell thickness. Thus, the motion of the fluid was neglected and the classical Laplace's formula was used. Whereas the actual curvature was taken into account in the motion plane, in the direction perpendicular to the flow the interface was assumed simply to be a half-circle with the diameter equal to the distance between the cell surfaces.

Obviously, expression (1.1) is the simplest and a rather rough assumption. A more rigorous condition should be sought by solving the equation for the motion of two fluids taking into account wettability of the walls, which have an influence on the shape of the moving interface. The authors of [10] performed such asymptotic analysis of the three-dimensional problem on a slow motion of the front of one fluid in another fluid at a velocity V_n. It was assumed that the latter fluid fully wetted the walls and left a thin film on the walls as it was displaced. The analysis led to the following approximate formula for the pressure jump:

$$\Delta p = 2\sigma/b + \alpha V_n^{\gamma} + \beta K, \tag{1.2}$$

where α, β and γ are some parameters (according to [10], $\alpha = 3.8\frac{2\sigma}{b}(\frac{\mu_2}{\sigma})^{\gamma}$, $\beta = \pi\sigma/4$ and $\gamma = 2/3$, where μ_2 is the viscosity of the displaced fluid). As distinct from (1.1), this expression explicitly takes into account the effect of the fluid velocity on the interface shape (the second term) and includes the correction for the change of the surface shape with the cell thickness (the third term).

A linear analysis of the stability in the case of the radial displacement was performed in [11–14] using the boundary condition (1.2) and taking into account finite boundaries of the cell. Results of these studies do not clarify the effect of the corrections in (1.2) on the stability since it was assumed, unlike in [8, 9], that the displacing fluid was injected at a constant pressure rather than at a constant velocity (volume flow rate). It is interesting to note also that, unlike in [8, 9], in studies [11–14] the interface always proved to be unstable to small perturbations of the translation type. A drawback of these studies is also the fact that the viscosity of the displacing fluid (and the size of the fluid source) was disregarded for simplicity of calculation. Therefore, the calculation results cannot be used for analysis of the motion of fluids having similar viscosities, but it is in this case, as we shall show below, that some interesting regularities are possible.

Thus, the above short review of past studies leads to the conclusion that the theoretical analysis of the linear stability of the radial displacement is far from complete. The full solution of this problem and its analysis are the objectives of the present study.

2. Problem statement

We shall consider a slow quasistationary displacement of a fluid by another fluid in the Hele–Shaw cell. Both fluids are assumed to be immiscible and incompressible. The motion is quasi-two-dimensional and all characteristics of the flow are averaged over the cell thickness (the third dimension—the cell thickness—is present only in (1.2)). These approximations are traditional for problems of this type [8–14].

The pressure field in both fluids satisfies the Laplace equation:

$$\nabla^2 p_1 = 0, \tag{2.1}$$

$$\nabla^2 p_2 = 0. \tag{2.2}$$

This is the consequence of the Darcy law $\boldsymbol{V}_i = -M_i \nabla p_i$ ($M_i = b^2/12\mu_i$, μ_i being the fluid viscosity) and the flow continuity condition $\nabla \boldsymbol{V}_i = 0$. Here p_i is the pressure in the fluid ($i = 1, 2$ for the displacing or the displaced fluid respectively) and $\boldsymbol{V}_i$ is the fluid velocity.

The pressures satisfy the following boundary conditions:

$$-M_1 \partial p_1/\partial \boldsymbol{n}|_{R_0} = \frac{Q}{2\pi R_0} \tag{2.3a}$$

or

$$p_1|_{R_0} = p_0, \tag{2.3b}$$

$$M_1 \partial p_1/\partial n|_r = M_2 \partial p_2/\partial n|_r, \tag{2.4}$$

$$p_1 - p_2|_r = \frac{2\sigma}{b} + \alpha V_n^{\gamma} + \beta K, \tag{2.5}$$

$$p_2|_{R_\infty} = 0, \tag{2.6}$$

where n is the normal to the surface; R_0 is the radius of the hole through which the displacing fluid is injected at a constant flow rate (Q, cm^2 s^{-1}) or a constant pressure (p_0, Pa); R_∞ is the size of the Hele–Shaw cell occupied by the displaced fluid; r is the equation for the interface of two fluids.

Equations (2.3a) and (2.3b) determine two basic methods of the displacement, namely, at a constant flow rate of the displacing fluid or at a constant pressure respectively. Equation (2.4) is the requirement for a continuous velocity of the fluids across the interface. Equation (2.5) is discussed in section 1. The pressure of the displaced fluid on the outer boundary of the cell is assumed to be constant (2.6) and zero for convenience of calculation (in this connection p_i can be taken as excess pressures relative to the external pressure).

We shall assume that an arbitrarily small distortion of the initially round interface can be presented as a superposition of harmonic functions of the form $\cos(n\varphi)$. Considering the linear order approximation, it suffices to discuss the behavior of one function so as to understand the stability of the front. In the polar system of coordinates the equation for the perturbed surface is written in the form

$$r = R + \delta\cos(n\varphi), \tag{2.7}$$

where R is the radius of the unperturbed surface; δ is the perturbation amplitude; n is the perturbation frequency (see figure 1); φ is the polar angle. The curvature in the linear order is given in the form

$$K = \frac{1}{R} + \frac{(n^2-1)}{R^2}\delta\cos(n\varphi). \tag{2.8}$$

In the boundary condition (2.4) $\partial p/\partial n$ can be written as components using the formula

$$\partial p/\partial \boldsymbol{n} = \nabla p \boldsymbol{e}_n,$$

where $\nabla p = \frac{\partial p}{\partial r}\boldsymbol{i}_r + \frac{1}{r}\frac{\partial p}{\partial \varphi}\boldsymbol{i}_\varphi$, $\boldsymbol{e}_n = \frac{\nabla\Phi}{|\nabla\Phi|}$, $\Phi = r - R - \delta\cos(n\varphi)$ and $\boldsymbol{e}_n$ is the unit normal to the surface $\Phi = 0$.

As a result, we can write with an accuracy of the first power of δ

$$\partial p/\partial n = \frac{1}{\sqrt{1 + (\delta n/r)^2\sin^2(n\varphi)}}\left(\frac{\partial p}{\partial r} + \frac{\delta n}{r^2}\frac{\partial p}{\partial \varphi}\sin(n\varphi)\right) \approx \left(\frac{\partial p}{\partial r} + \frac{\delta n}{r^2}\frac{\partial p}{\partial \varphi}\sin(n\varphi)\right). \tag{2.9}$$

Using (2.9) and the Darcy law, we can write

$$V_n|_r = -M_i\left(\frac{\partial p_i}{\partial r}\bigg|_r + \frac{\delta n}{r^2}\frac{\partial p_i}{\partial \varphi}\sin(n\varphi)\bigg|_r\right). \tag{2.10}$$

3. Solution of the problem on the linear stability of the front

Represent the pressure as a power series of δ:

$$p_i(r,\varphi) = p_i^0(r) + p_i^1(r,\varphi)\delta. \tag{3.1}$$

The expression (2.10) can be expanded near the boundary R. Then in the linear order we have

$$V_n|_{R+\delta\cos(n\varphi)} = -M_i\left(\left.\frac{\partial p_i^0}{\partial r}\right|_R + \left.\frac{\partial^2 p_i^0}{\partial r^2}\right|_R \delta\cos(n\varphi) + \left.\frac{\partial p_i^1}{\partial r}\right|_R \delta\right), \tag{3.2}$$

$$V_n^\gamma|_{R+\delta\cos(n\varphi)} = \left(-M_i\left.\frac{\partial p_i^0}{\partial r}\right|_R\right)^\gamma \left[1+\gamma\left(\frac{\left.\partial^2 p_i^0/\partial r^2\right|_R}{\left.\partial p_i^0/\partial r\right|_R}\times\delta\cos(n\varphi) + \frac{\left.\partial p_i^1/\partial r\right|_R}{\left.\partial p_i^0/\partial r\right|_R}\delta\right)\right]. \tag{3.3}$$

Substitute (3.1) and (3.3) into equations (2.1)–(2.6) and expand the terms in (2.4) and (2.5) into a Taylor series near R. Then, equating the coefficients in the expressions at the zeroth and the first order in δ, we obtain two sets of equations for calculation of p_i^0 and p_i^1:

(1)

$$\nabla^2 p_1^0 = 0, \tag{3.4}$$

$$\nabla^2 p_2^0 = 0. \tag{3.5}$$

With boundary conditions

$$-M_1\left.\frac{\partial p_1^0}{\partial r}\right|_{R_0} = \frac{Q}{2\pi R_0} \tag{3.6a}$$

or

$$\left.p_1^0\right|_{R_0} = p_0, \tag{3.6b}$$

$$M_1\left.\frac{\partial p_1^0}{\partial r}\right|_R = M_2\left.\frac{\partial p_2^0}{\partial r}\right|_R, \tag{3.7}$$

$$p_1^0 - p_2^0|_R = \frac{2\sigma}{b} + \frac{\beta}{R} + \alpha\left(-M_2\left.\frac{\partial p_2^0}{\partial r}\right|_R\right)^\gamma, \tag{3.8}$$

$$\left.p_2^0\right|_{R_\infty} = 0, \tag{3.9}$$

(2)

$$\nabla^2 p_1^1 = 0, \tag{3.10}$$

$$\nabla^2 p_2^1 = 0. \tag{3.11}$$

With boundary conditions

$$M_1\left.\frac{\partial p_1^1}{\partial r}\right|_{R_0} = 0 \tag{3.12a}$$

or

$$\left.p_1^1\right|_{R_0} = 0, \tag{3.12b}$$

$$M_1\left(\left.\frac{\partial^2 p_1^0}{\partial r^2}\right|_R\cos(n\varphi) + \left.\frac{\partial p_1^1}{\partial r}\right|_R\right) = M_2\left(\left.\frac{\partial^2 p_2^0}{\partial r^2}\right|_R\cos(n\varphi) + \left.\frac{\partial p_2^1}{\partial r}\right|_R\right), \tag{3.13}$$

$$\left(\left.\frac{\partial p_1^0}{\partial r}\right|_R - \left.\frac{\partial p_2^0}{\partial r}\right|_R\right)\cos(n\varphi) + \left(p_1^1|_R - p_2^1|_R\right) = \gamma\alpha\left(-M_2\left.\frac{\partial p_2^0}{\partial r}\right|_R\right)^\gamma\left(\frac{\left.\partial^2 p_2^0/\partial r^2\right|_R}{\left.\partial p_2^0/\partial r\right|_R}\cos(n\varphi) + \frac{\left.\partial p_2^1/\partial r\right|_R}{\left.\partial p_2^0/\partial r\right|_R}\right) + \frac{\beta(n^2-1)}{R^2}\cos(n\varphi), \tag{3.14}$$

$$\left.p_2^1\right|_{R_\infty} = 0. \tag{3.15}$$

The general solution of the Laplace equations (3.4)–(3.5) and (3.10)–(3.11) in the zeroth and the first order is written respectively as

$$p_i^0(r) = A_i^0\ln(r) + B_i^0, \tag{3.16}$$

$$p_i^1(r,\varphi) = A_i^1\ln(r) + B_i^1 + r^n(a_i\cos(n\varphi) + b_i\sin(n\varphi)) + r^{-n}(c_i\cos(n\varphi) + d_i\sin(n\varphi)). \tag{3.17}$$

3.1. A constant flow rate of the injected fluid

Substituting (3.16)–(3.17) into (3.4)–(3.6*a*), (3.7)–(3.12*a*) and (3.13)–(3.15) and equating the terms at the corresponding powers of the cosines and the sines, it is possible to determine the unknown coefficients in (3.16)–(3.17), some of which (A_i^1, B_i^1, b_i, d_i) prove to be zero. As a result, the solution is written as

$$p_1^0 = -\frac{Q}{2\pi M_1}\ln(r/R) - \frac{Q}{2\pi M_2}\ln(R/R_\infty) + \frac{2\sigma}{b} + \frac{\beta}{R} + \alpha\left(\frac{Q}{2\pi R}\right)^\gamma, \tag{3.18}$$

$$p_2^0 = -\frac{Q}{2\pi M_2}\ln(r/R_\infty), \tag{3.19}$$

$$p_1^1 = a_1 r^n\cos(n\varphi)[1+(R_0/r)^{2n}], \tag{3.20}$$

$$p_2^1 = a_2 r^n\cos(n\varphi)[1-(R_\infty/r)^{2n}], \tag{3.21}$$

where

$$a_1 = R^{-n}\left[\frac{Q}{2\pi R}\frac{M_2-M_1}{M_1M_2} + \frac{\beta(n^2-1)}{R^2} - \frac{\alpha\gamma}{R}\left(\frac{Q}{2\pi R}\right)^\gamma\right] \times\left[\left[1+(R_0/R)^{2n}\right] + \frac{M_1}{M_2}\frac{1-(R/R_\infty)^{2n}}{1+(R/R_\infty)^{2n}} \times[1-(R_0/R)^{2n}] + \alpha\gamma n\left(\frac{Q}{2\pi R}\right)^\gamma\frac{2\pi M_1}{Q} \times\left[1-(R_0/R)^{2n}\right]\right]^{-1}$$

$$a_2 = R^{-n}\left[\frac{Q}{2\pi R}\frac{M_2-M_1}{M_1M_2} + \frac{\beta(n^2-1)}{R^2} - \frac{\alpha\gamma}{R}\left(\frac{Q}{2\pi R}\right)^\gamma\right] \times\left[\frac{M_2}{M_1}\frac{1+(R_0/R)^{2n}}{1-(R_0/R)^{2n}}\left[1+(R_\infty/R)^{2n}\right] - [1-(R_\infty/R)^{2n}] + \alpha\gamma n\left(\frac{Q}{2\pi R}\right)^\gamma\frac{2\pi M_2}{Q} \times\left[1+(R_\infty/R)^{2n}\right]\right]^{-1}.$$

Let us determine the stability radius of the interface. For this purpose, substitute (3.18)–(3.21) into (3.2). Write the

interface velocity in the form

$$V_n\big|_{R+\delta\cos(n\varphi)} = \dot{R} + \dot{\delta}\cos(n\varphi), \tag{3.22}$$

where $\dot{R}$ is the velocity of the unperturbed interface and $\dot{\delta}$ is the perturbation growth rate. Grouping the terms at the corresponding powers of δ, we can write

$$\dot{R} = Q/2\pi R, \tag{3.23}$$

$$\frac{\dot{\delta}/\delta}{\dot{R}/R} = -1 - n\left(\frac{M_2}{M_1} - 1\right) \times \left[1 + \left((n^2-1)\frac{\beta}{R} - \alpha\gamma\left(\frac{Q}{2\pi R}\right)^{\gamma}\right)\frac{2\pi}{Q}\frac{M_1M_2}{M_2 - M_1}\right] \times \left[\frac{M_2}{M_1}\frac{1+(R_0/R)^{2n}}{1-(R_0/R)^{2n}} + \frac{1-(R/R_\infty)^{2n}}{1+(R/R_\infty)^{2n}} + n\alpha\gamma\left(\frac{Q}{2\pi R}\right)^{\gamma}\frac{2\pi M_2}{Q}\right]^{-1}. \tag{3.24}$$

Notice that at $R_\infty \to \infty$, $R_0 \to 0$, $\alpha = 0$ and $\beta = \sigma$ expression (3.24) coincides with the classical expression given in [9].

The critical size of the interface stability R_S when the perturbation growth rate $\dot{\delta}$ reverses sign from negative (damping) to positive (growth) can be determined from the equation

$$\frac{\dot{\delta}/\delta}{\dot{R}/R} = 0 \tag{3.25}$$

by solving it for R.

3.2. A constant pressure of the injected fluid

The solution is similar to the one described above (the only difference is the boundary conditions (3.6*b*) and (3.12*b*)). As a result, it is possible to determine the pressure of each fluid.

For the zero order

$$p_1^0 = (M_2/M_1)C_0\ln(r/R_0) + p_0, \tag{3.26}$$

$$p_2^0 = C_0\ln(r/R_\infty), \tag{3.27}$$

where C_0 satisfies the equation

$$C_0^{\gamma}\alpha\,(-M_2/R)^{\gamma} - C_0\left[(M_2/M_1)\,\ln(R/R_0) - \ln(R/R_\infty)\right] + 2\sigma/b + \beta/R - p_0 = 0. \tag{3.28}$$

For the first order

$$p_1^1 = a_1 r^n\cos(n\varphi)[1-(R_0/r)^{2n}], \tag{3.29}$$

$$p_2^1 = a_2 r^n\cos(n\varphi)[1-(R_\infty/r)^{2n}], \tag{3.30}$$

where

$$a_1 = R^{-n}\left[-\frac{C_0}{R}\frac{M_2-M_1}{M_1} + \frac{\beta(n^2-1)}{R^2} - \frac{\alpha\gamma}{R}\left(-\frac{M_2C_0}{R}\right)^{\gamma}\right] \times \left[\left[1-(R_0/R)^{2n}\right] + \frac{M_1}{M_2}\frac{1-(R/R_\infty)^{2n}}{1+(R/R_\infty)^{2n}} \times \left[1+(R_0/R)^{2n}\right] - \frac{M_1}{M_2}\frac{\alpha\gamma n}{C_0}\left(-\frac{M_2C_0}{R}\right)^{\gamma} \times \left[1+(R_0/R)^{2n}\right]\right]^{-1}$$

$$a_2 = R^{-n}\left[-\frac{C_0}{R}\frac{M_2-M_1}{M_1} + \frac{\beta(n^2-1)}{R^2} - \frac{\alpha\gamma}{R}\left(-\frac{M_2C_0}{R}\right)^{\gamma}\right]\left[\frac{M_2}{M_1}\frac{1-(R_0/R)^{2n}}{1+(R_0/R)^{2n}} \times \left[1+(R_\infty/R)^{2n}\right] - \left[1-(R_\infty/R)^{2n}\right] - \frac{\alpha\gamma n}{C_0} \times \left(-\frac{M_2C_0}{R}\right)^{\gamma}\left[1+(R_\infty/R)^{2n}\right]\right]^{-1}.$$

Substituting (3.26), (3.27), (3.29) and (3.30) into (3.2), we have

$$\dot{R} = -M_2C_0/R, \tag{3.31}$$

$$\frac{\dot{\delta}/\delta}{\dot{R}/R} = -1 - n\left(\frac{M_2}{M_1} - 1\right)\left[1 - \left((n^2-1)\frac{\beta}{RC_0} - \alpha\gamma\,(-M_2/R)^{\gamma}\,C_0^{\gamma-1}\right) \times \frac{M_1}{M_2-M_1}\right]\left[\frac{M_2}{M_1}\frac{1-(R_0/R)^{2n}}{1+(R_0/R)^{2n}} + \frac{1-(R/R_\infty)^{2n}}{1+(R/R_\infty)^{2n}} - n\alpha\gamma\,(-M_2/R)^{\gamma}\,C_0^{\gamma-1}\right]^{-1}. \tag{3.32}$$

Similar calculations were performed in [11–14], but the viscosity of the displacing fluid and the size of the fluid source were disregarded. Also, it was assumed that $\gamma = 1$ [11, 12] and $\beta = \sigma$ [11–14] in (2.5), considerably simplifying the solution. If all the aforementioned simplifications are taken into account, (3.32) transforms to the solutions given in [11–14].

4. Analysis of results

4.1. A constant flow rate of the injected fluid

As discussed in section 3.1, the critical size R_S of the linear stability of the interface between two fluids can be found by solving equation (3.25) for R. This cannot be done analytically. Therefore, a numerical analysis was performed and main results of this analysis are discussed below.

Figure 2(a) shows R_S as a function of the cell size R_∞. It is seen that R_S grows and quickly reaches saturation as R_∞ increases. The inset presents the difference between the calculated critical radius and the radius calculated in [9] using boundary condition (1.1) instead of (1.2) and the assumption of infinite size of the cell. It is seen that, although the results approach as R_∞ increases, the approximation [8, 9] can lead to highly overestimated (up to 30 percent) values at the size of the fluid source and the cell used in the experiments.

The calculations in figure 3(a) demonstrate that the critical size of the stability decreases with increasing flow rate. This is a direct indication that the degree of the system nonequilibrium is the reason for the instability. It can also be shown numerically that the stabilizing factor is the surface tension and the instability is observed only when a less viscous fluid displaces a more viscous fluid ($M_1 > M_2$).[1]

[1] A more mobile and less inert fluid tends to outrun the other fluid during their motion under the action of the pressure gradient. This is very much like the case if two fluids having different densities are placed in the gravity field—the situation is unstable only if the less inert/dense fluid is below.

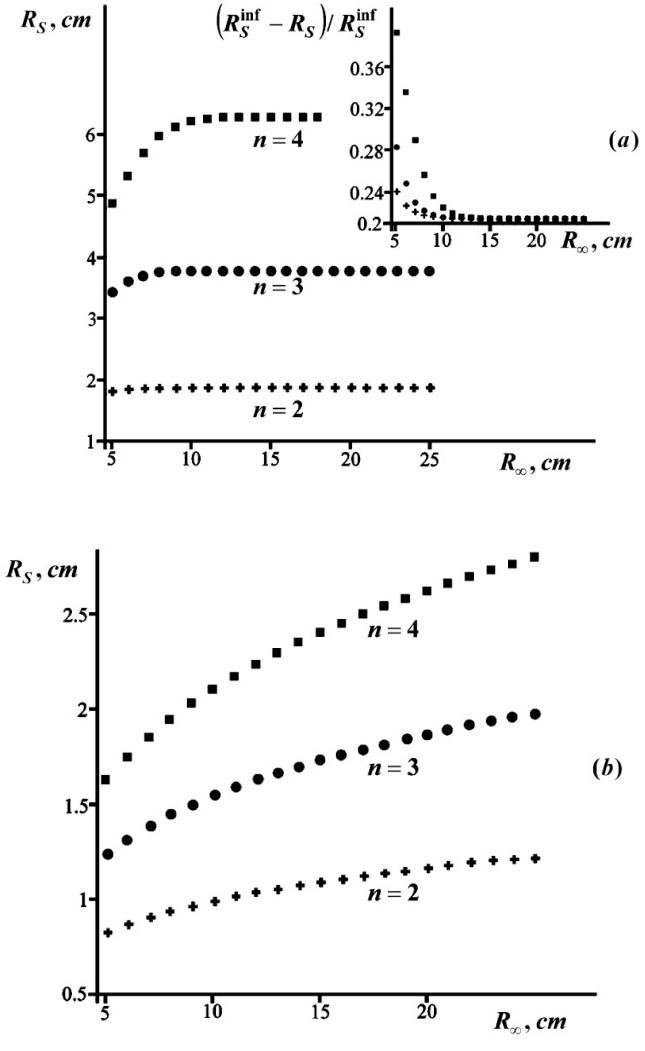

Figure 2. Dependence of the critical radius R_S on the cell size R_∞ at (a) a constant volume flow rate $Q \times b = 0.06$ ml s^{-1} (the insets show the dependence of the relative deviation of the critical radius R_S from the critical radius R_S^{inf} found on the assumption of $R_\infty \to \infty$ [8, 9]) and (b) a constant pressure $p_0 = 85$ Pa. The curves were plotted taking $R_0 = 2$ mm, $b = 1, 5$ mm, $\sigma = 31.3 \times 10^{-3}$ N m^{-1}, $\mu_1 = 1.72 \times 10^{-5}$ kg m^{-1} s^{-1} and $\mu_2 = 230 \times 10^{-3}$ kg m^{-1} s^{-1} (the viscosity and the surface tension correspond to those of air and castor oil).

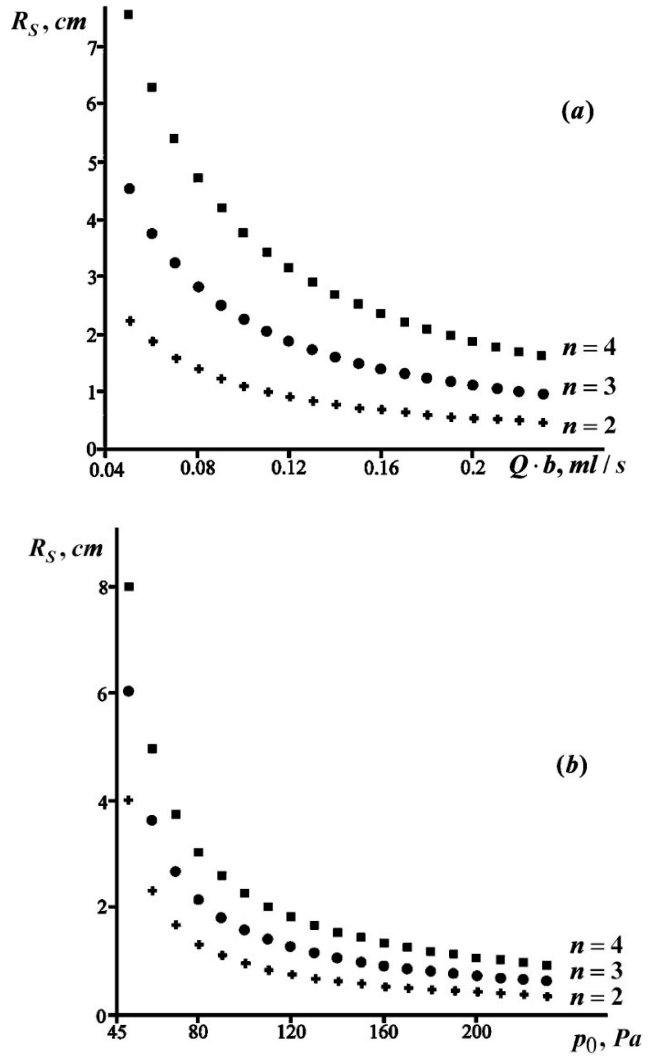

Figure 3. Dependence of the critical radius R_S on (a) the volume flow rate Qb and (b) the source pressure p_0. The curves were plotted taking the same parameters as in figure 2, $R_\infty = 15$ cm.

Of special interest is the case when the perturbation frequency n equals unity (a perturbation of the translation type). Here formula (3.24) is considerably simplified and the critical radius can be expressed explicitly:

$$R_S = R_0 \left[\frac{(M_2/M_1)(R_\infty/R_0)^2 + 1}{1 - M_2/M_1} \right]^{1/2}. \qquad (4.1)$$

Notice first that when $R_\infty \to \infty$ and $R_0 \to 0$, in line with (4.1) R_S tends to infinity and the system is stable with respect to translation. This limit was considered in [8, 9]. When finiteness of the cell is introduced, the reason for the instability is that only in this case an asymmetry appears in the system during translation of the displaced fluid relative to the center of the system: the pressure differential is larger in the displacement direction and smaller in the opposite direction. Consequently, a positive feedback is formed between the motive force and the displacement, leading to further development of the instability.

According to (4.1), the most important parameter influencing the critical radius of the translation stability is the viscosity ratio M_2/M_1. If $M_2/M_1 = 0$, the interface becomes unstable immediately at the hole exit and the region of the linear instability of the interface (R_0, R_S) is expanded rather quickly (see also figures 4 and 5) with increasing M_2/M_1. It should be noted in this connection (see the insets in figures 4 and 5) that the translation instability dominates in the development of the interface (at the perturbation with $n = 1$ R_S is the smallest as compared with its values at perturbations with other n) if the viscosity of the displacing fluid is much lower than the viscosity of the displaced fluid (e.g. when gas displaces a fluid).

Instabilities due to harmonics with $n > 1$ become dominant starting from some M_2/M_1 values. As can be seen from figures 4 and 5, the viscosity ratio can be selected such that the system will not undergo the instability with respect

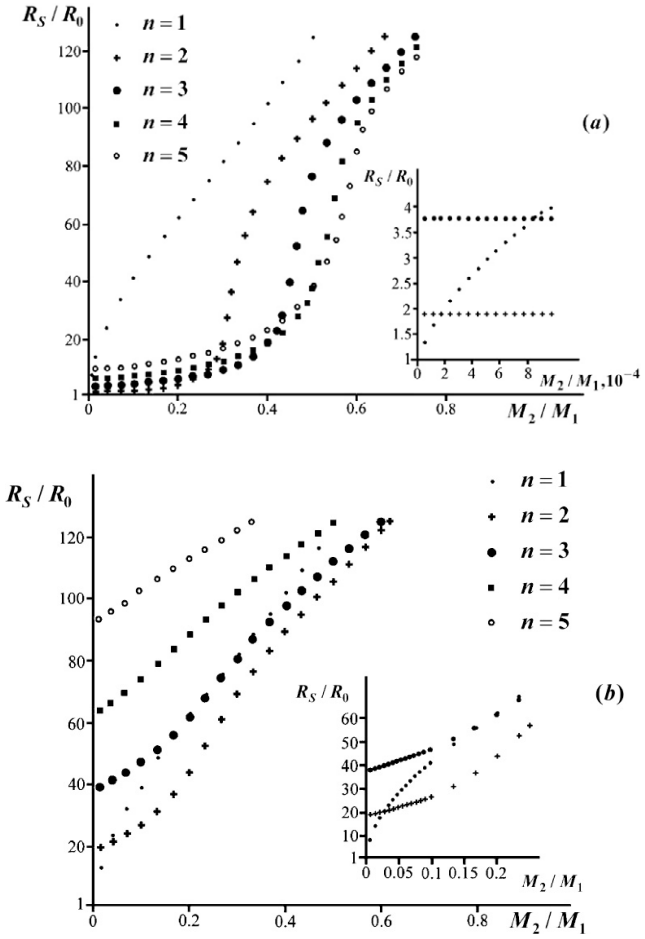

Figure 4. Dependence of R_S/R_0 on M_2/M_1 at (a) $\beta M_2/Q = 10^{-4}$ m and (b) $\beta M_2/Q = 10^{-3}$ m. The curves were plotted taking $R_\infty = 25$ cm and $R_0 = 2$ mm.

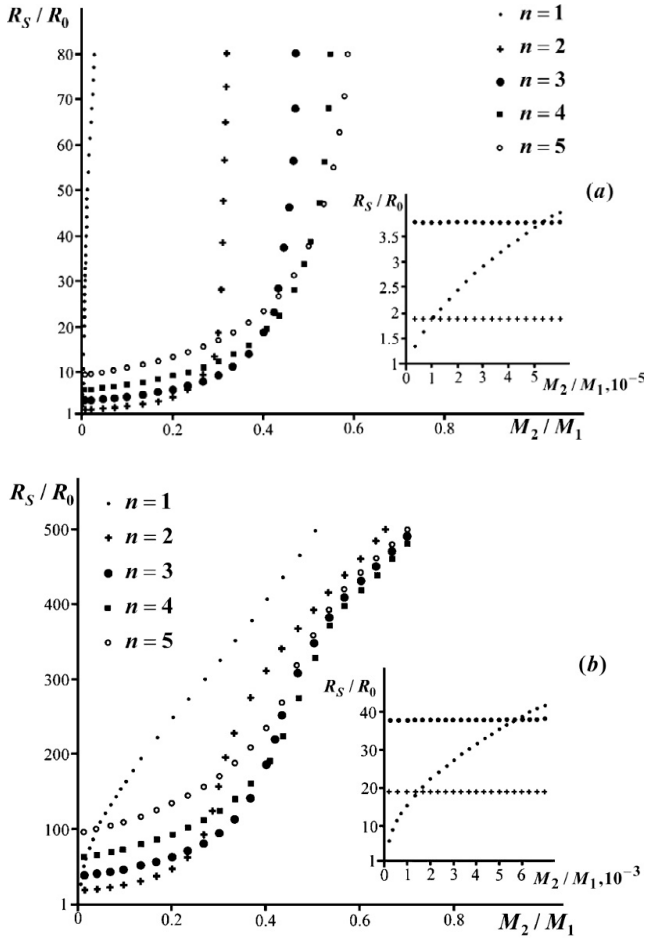

Figure 5. Dependence of R_S/R_0 on M_2/M_1 at (a) $\beta M_2/Q = 10^{-4}$ m and (b) $\beta M_2/Q = 10^{-3}$ m. The curves were plotted taking $R_\infty = 100$ cm and $R_0 = 2$ mm.

to the first harmonic and will lose its stability immediately with respect to the second harmonic. If M_2/M_1 increases further, the third, the fourth, the fifth etc harmonics are put to the forefront. Thus, according to the numerical calculations, the ratio of the fluid viscosities can be selected such that the stability is lost starting from an arbitrary number of the perturbation frequency.

This feature is very interesting from the viewpoint of the theory and experimental applications. Therefore, for complete analysis it seems reasonable to solve this problem analytically at least for some instances allowing calculations in the general form. We shall take the approximations used in [9], i.e. $R_\infty \to \infty$ and $R_0 \to 0$, $\alpha = 0$ and $\beta = \sigma$. Then (3.24) is rearranged to the form

$$\frac{\dot\delta/\delta}{\dot R/R} = n\frac{1 - M_2/M_1}{1 + M_2/M_1} - 1 - n(n^2 - 1) \times \frac{2\pi\sigma}{QR}\frac{M_2}{1 + M_2/M_1}. \tag{4.2}$$

The critical size of the stability loss can be expressed explicitly from expression (4.2):

$$R_S = \frac{n(n^2 - 1)\frac{2\pi\sigma}{Q}\frac{M_2}{1+M_2/M_1}}{n\frac{1-M_2/M_1}{1+M_2/M_1} - 1}. \tag{4.3}$$

The R_S value should be positive and, according to (4.3), this is possible only if the condition

$$M_2/M_1 < (n - 1)/(n + 1) \tag{4.4}$$

is fulfilled.

It follows from (4.2) that if condition (4.4) is not met, $\dot\delta$ is negative at any R, i.e. the system is stable with respect to the nth harmonic. Using (4.3) we can find the viscosity ratio at which the instability takes place at one and the same R_S with respect to two arbitrary perturbation frequencies n_1 and n_2 (essentially the intersections of the curves in figures 4 and 5)

$$\frac{n_1(n_1^2 - 1)}{n_1\frac{1-M_2/M_1}{1+M_2/M_1} - 1} = \frac{n_2(n_2^2 - 1)}{n_2\frac{1-M_2/M_1}{1+M_2/M_1} - 1}$$

or after the rearrangement

$$\frac{M_2}{M_1} = \frac{n_1n_2(n_2^2 - n_1^2) - n_2(n_2^2 - 1) + n_1(n_1^2 - 1)}{n_1n_2(n_2^2 - n_1^2) + n_2(n_2^2 - 1) - n_1(n_1^2 - 1)}. \tag{4.5}$$

Let $n_2 > n_1$, then in accordance with (4.4) we can write

$$\frac{M_2}{M_1} < \frac{n_1 - 1}{n_1 + 1} < \frac{n_2 - 1}{n_2 + 1}.$$

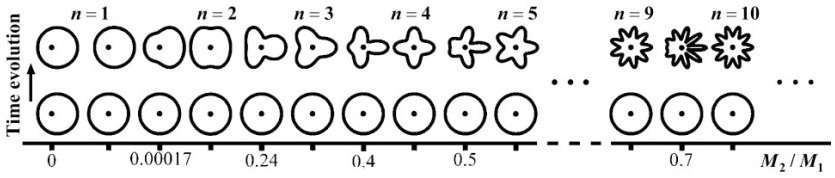

Figure 6. Possible sequence of structures during displacement in the Hele–Shaw cell at different viscosity ratios M_2/M_1. The parameters are similar to those used in figure 4 (a).

It can be concluded from the last inequality and (4.5) that if n_1 is fixed the perturbation frequency n_2 can acquire values at which the relationship

$$\frac{n_1 n_2(n_2^2 - n_1^2) - n_2(n_2^2 - 1) + n_1(n_1^2 - 1)}{n_1 n_2(n_2^2 - n_1^2) + n_2(n_2^2 - 1) - n_1(n_1^2 - 1)} < \frac{(n_1 - 1)}{(n_1 + 1)} \tag{4.6}$$

is fulfilled.

Rearrangement of (4.6) gives

$$(n_1^2 - 1)(n_2 - n_1) > 0. \tag{4.7}$$

The last inequality is fulfilled at all $n_2 > n_1$ ($n_1 > 1$). It follows from the above discussion that the critical radius at an arbitrary n_2 becomes equal to the critical radius at the perturbation with n_1 as M_2/M_1 increases. Let us dwell on this point in more detail. In accordance with (4.3), a larger critical radius corresponds to larger n ($n \neq 1$) at small M_2/M_1. As M_2/M_1 increases, the growth of R_S becomes considerably nonlinear; the smaller n, the earlier and the more prominent is the nonlinearity. As a result, the interface becomes stable with respect to long-wave perturbations and less stable to short-wave perturbations.

As the above calculations indicate (figures 4 and 5), the analytically detected regularity is preserved when the cell size is taken into account and a more correct boundary condition is used; however, the intersections depend not only on M_2/M_1, but also on $\beta M_2/Q$ and R_∞ (the effect of R_0 is negligibly small). The comparison of figures 4(a) and (b) shows that if the cell size R_∞ is relatively small the increase in $\beta M_2/Q$ leads not only to the growth of R_S but also to the displacement of intersections towards larger M_2/M_1. Thus, $\beta M_2/Q$ can be selected such that all or part of the curves intersect or do not intersect at all. Then it is possible to control the sequence of nonequilibrium transitions from the stable to the unstable growth under the action of perturbations having different frequencies n. One of the possible instances of the interface evolution is shown in figure 6. A similar conclusion is true for the second control parameter R_∞ (compare, e.g., figures 4 and 5). Notice that at sufficiently large R_∞ the effect of $\beta M_2/Q$ on the intersections is weak (compare figures 5(a) and (b)).

4.2. Displacement at a constant pressure

Results of the numerical analysis (3.32) (see figures 2(b), 3(b) and 7) demonstrate that the majority of the phenomena discussed in section 4.1 are also observed during displacement at a constant pressure. For this reason, in what follows we only present some interesting distinctions.

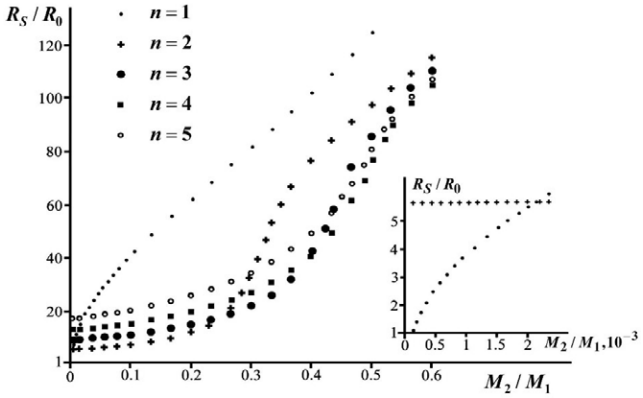

Figure 7. Dependence of R_S/R_0 on M_2/M_1 at $p_0 = 90$ Pa. The curves were plotted taking $R_\infty = 25$ cm, $R_0 = 2$ mm, $b = 1.5$ mm, $\sigma = 31.3 \times 10^{-3}$ N m^{-1} and $\mu_2 = 230 \times 10^{-3}$ kg m^{-1} s^{-1}.

(1) The comparison of figures 2(a) and (b) shows that in this case R_S is not saturated, but increases permanently. This distinction can be explained by the fact that at $p_0 = \text{const}$ the increase in the size leads to the continuous decrease in the motive force of the displacement (and the instability), that is, the pressure differential[2] (approximately equal to $p_0/(R_\infty - R_0)$).

(2) In the case of the translation instability at a constant pressure the critical radius is given by

$$R_S = R_0 \left[\frac{(M_2/M_1)(R_\infty/R_0)^2 - 1}{1 - M_2/M_1} \right]^{1/2}. \tag{4.8}$$

The effect of the boundary on the translation stability is described in [11–14]. However, these studies have a considerable drawback, that the viscosity of the displacing fluid is neglected in the solution. As a result, the system is always unstable with respect to the first-harmonic perturbation from the very beginning of the displacement process at any small viscosity ratio. It follows from our calculations (3.32) and (4.8) that at $M_2/M_1 \leqslant (R_0/R_\infty)^2$ this conclusion holds. However, at $M_2/M_1 > (R_0/R_\infty)^2$ there is some region of large R_0 when the interface is always translation stable. Different behaviors of the critical radius ($n = 1$, M_2/M_1 is small) at $Q = \text{const}$ and $p_0 = \text{const}$ are apparent from the comparison of the insets in figures 4 and 7.

(3) The dependence of R_S/R_0 on M_2/M_1 at a constant pressure (figure 7) is qualitatively similar to the dependence in figure 4.

[2] This unique relationship between the displacement force and the size of the system is not observed at a constant flow rate.

(4) As M_2/M_1 increases, the interface becomes more stable to long-wave perturbations and less stable to short-wave perturbations. However, the intersections of the critical radii related to different n depend on a much larger number of the problem parameters (α, β, γ, M_2, M_2/M_1, b, R_∞,R_0) which cannot be grouped to a smaller number of complexes (as in the case of $Q = \text{const}$).

5. Conclusion

The stability of the radial displacement front in the Hele–Shaw cell was calculated at a constant flow rate or a constant pressure. Unlike in other studies, the finite size of the cell and the nonzero viscosity of the displacing fluid were taken into account. In addition to a considerable quantitative refinement of the results, at least two interesting phenomena were predicted.

(1) It was found that the sensitivity of the system to the perturbation of the translation type depends on the ratio of viscosities of the displaced and displacing fluids and the cell size. These parameters can be selected such that the system is stable or unstable to this type of perturbation.
(2) One more interesting phenomenon consists in that any mode can be made the first unstable mode if we properly select the ratio of the fluid viscosities or some other parameters. In other words, the system will be especially sensitive to perturbations having a certain frequency and insensitive to the other noise present in the system.

Acknowledgment

This work was partially supported by the Russian Foundation for Basic Research (grant No 070800-139).

References

[1] Saffman P G and Taylor G 1958 The penetration of a fluid into a porous medium or Hele–Shaw cell containing a more viscous liquid *Proc. R. Soc.* A **245** 312–29
[2] Bensimon D, Kadanoff L P, Liang S, Shraiman B I and Chao T 1986 Viscous flows in two dimensions *Rev. Mod. Phys.* **58** 977–99
[3] Homsy G M 1987 Viscous fingering in porous media *Ann. Rev. Fluid Mech.* **19** 271–311
[4] Kessler D A, Koplik J and Levin H 1988 Pattern selection in fingered growth phenomena *Adv. Phys.* **37** 255–339
[5] Cummings L J, Howison S D and King J R 1999 Two-dimensional Stokes and Hele–Shaw flows with free surfaces *Eur. J. Appl. Math.* **10** 635–80
[6] Chevalier C, Ben Amar M, Bonn D and Lindner A 2006 Inertial effects on Saffman–Taylor viscous fingering *J. Fluid Mech.* **552** 83–97
[7] Lindner A, Bonn D, Poire E C, Ben Amar M and Meunier J 2002 Viscous fingering in non-Newtonian fluids *J. Fluid Mech.* **469** 237–56
[8] Wilson S D R 1975 A note of the measurement of dynamic contact angles *J. Colloid Interface Sci.* **51** 532–4
[9] Paterson L 1981 Radial fingering in a Hele Shaw cell *J. Fluid Mech.* **113** 513–29
[10] Park C-W and Homsy G M 1984 Two-phase displacement in Hele Shaw cells: theory *J. Fluid Mech.* **139** 291–308
[11] Ben-Jacob E, Deutscher G and Garik P *et al* 1986 Formation of a dense branching morphology in interfacial growth *Phys. Rev. Lett.* **57** 1903–6
[12] Ben-Jacob E and Garik P 1989 Ordered shapes in nonequilibrium growth *Physica* D **38** 16–28
[13] Buka A and Palffy-Muhoray P 1987 Stability of viscous fingering patterns in liquid crystals *Phys. Rev.* A **36** 1527–9
[14] Buka A, Palffy-Muhoray P and Racz Z 1987 Viscous fingering in liquid crystals *Phys. Rev.* A **36** 3984–9